



Contents lists available at ScienceDirect

Journal of Traditional and Complementary Medicine

journal homepage: <http://www.elsevier.com/locate/jtcme>

Orengedokuto and san'oshashinto improve memory deficits by inhibiting aging-dependent activation of glycogen synthase kinase-3 β

Hironori Fujiwara ^{a,*}, Jun Yoshida ^a, Dya Fita Dibwe ^a, Suresh Awale ^a, Haruka Hoshino ^a, Hiroshi Kohama ^a, Hiroyuki Arai ^b, Yukitsuka Kudo ^b, Kinzo Matsumoto ^a

^a Institute of Natural Medicine, University of Toyama, Toyama, Japan

^b Department of Geriatric and Respiratory Medicine, Institute of Development, Aging and Cancer, Tohoku University, Sendai, Japan

ARTICLE INFO

Article history:

Received 19 June 2018

Received in revised form

20 December 2018

Accepted 26 December 2018

Available online 27 December 2018

Keywords:

Alzheimer's disease

Glycogen synthase kinase-3 β

Collapsin response mediator protein-2

Orengedokuto

san'oshashinto

ABSTRACT

Background and aim: The aging-dependent activation of glycogen synthase kinase-3 β (GSK-3 β) has been suggested to be important in the onset of dementia. To discover novel therapeutic kampo medicines for dementia, we examined the effects of orengedokuto (OGT; 黃連解毒湯 *huáng lián jiědú tāng*) and san'oshashinto (SST; 三黃瀉心湯 *sān huáng xiè xīn tāng*) on memory deficits and GSK-3 β activity in senescence-accelerated prone mice (SAMP8).

Experimental procedure: The object recognition test (ORT) and conditioned fear memory test (CFT) were employed to elucidate short-term working memory and long-term fear memory. The activity of GSK-3 β and the phosphorylation of related molecules were measured using a kinase assay and Western blotting. **Results and conclusion:** OGT and SST attenuated memory deficits in SAMP8 in ORT, but not in CFT. In *ex vivo* experiments, cortical GSK-3 β activity was significantly stronger in SAMP8 than in SAMR1. The enhanced cortical GSK-3 β activity in SAMP8 was accompanied by a significant increase in the level of phosphorylated collapsin response mediator protein-2 (CRMP2), an important factor that is involved in the regulation of microtubule stability. OGT and SST attenuated not only increases in cortical GSK-3 β activity, but also the levels of phosphorylated CRMP2 in SAMP8. In vitro experiments, flavonoids contained in these kampo medicines, inhibited GSK-3 β activity in concentration-dependent manners. These results suggest that OGT and SST prevent aging-induced short-term working memory deficits by inhibiting aging-dependent elevations in the cortical GSK-3 β activity and subsequent CRMP2 phosphorylation.

© 2019 Center for Food and Biomolecules, National Taiwan University. Production and hosting by Elsevier Taiwan LLC. This is an open access article under the CC BY-NC-ND license (<http://creativecommons.org/licenses/by-nc-nd/4.0/>).

1. Introduction

Alzheimer's disease (AD) is one of the causative diseases of dementia and is accompanied by memory and cognition deficits in addition to the behavioral and psychological symptoms of

Abbreviations: AD, Alzheimer's disease; BPSD, behavioral and psychological symptoms of dementia; CFT, conditioned fear memory test; CRMP2, collapsin response mediator protein-2; GSK-3 β , glycogen synthase kinase-3 β ; OGT, orengedokuto; ORT, object recognition test; SAMP8, senescence-accelerated prone mice 8; SAMR1, senescence-accelerated prone mice-resistant; SST, san'oshashinto.

* Corresponding author. Institute of Natural Medicine, University of Toyama, Toyama, 2630 Sugitani, Toyama, 930-0194, Japan.

E-mail address: arawijuf@inm.u-toyama.ac.jp (H. Fujiwara).

Peer review under responsibility of The Center for Food and Biomolecules, National Taiwan University.

<https://doi.org/10.1016/j.jtcme.2018.12.001>

2225-4110/© 2019 Center for Food and Biomolecules, National Taiwan University. Production and hosting by Elsevier Taiwan LLC. This is an open access article under the CC BY-NC-ND license (<http://creativecommons.org/licenses/by-nc-nd/4.0/>).

dementia (BPSD). There are two pathological characteristics of AD: the deposition of insoluble senile plaques composed of amyloid- β protein¹ and the intracellular accumulation of neurofibrillary tangles composed of tau-based paired helical filaments.² Hyperphosphorylated tau protein is a main component of neurofibrillary tangles. Tau protein normally binds to microtubules, thereby contributing to cytoskeleton stabilization; however, once hyperphosphorylated by several serine-threonine kinases such as glycogen synthase kinase-3 β (GSK-3 β), cyclin-dependent kinase-5, and mitogen-activated protein kinase,^{3,4} it dissociates from microtubules. GSK-3 β is involved in the onset of various diseases such as neuropathy, inflammatory disease, and cancer.^{5–8} GSK-3 β is generally phosphorylated by other kinases to its inactive state, and is activated by the inhibition of phosphorylation, which occurs under pathological conditions.⁹ The activity of GSK-3 β in the brain increases with aging,¹⁰ and the expression level and activity of GSK-

β were found to be elevated in the brains of type II diabetic patients with mild cognitive impairment.¹¹ Based on these findings, we hypothesized that the regulation of GSK-3 β activity represents an important strategy for effective therapy for dementia.

Collapsin response mediator protein-2 (CRMP2) is a member of the collapsin response mediator protein family. This protein is strongly expressed in the nervous system and is involved in kinesin-dependent axonal transport, neurite outgrowth and retraction, and microtubule dynamics.^{12,13} Similar to tau protein, CRMP2 is phosphorylated at the Thr509 and Thr514 residues by GSK-3 β . This process reduces the binding affinity of CRMP2 for tubulin, resulting in the destabilization of microtubules.^{14,15} Synaptic deficits and the accumulation of phosphorylated CRMP2 have been reported in the brains of patients with dementia^{16,17} as well as in those of AD model animals.¹⁸ An increase in the phosphorylated form of CRMP2 as well as in synaptic dysfunction may occur in the early stage of AD.

Recent clinical studies on AD patients showed that some Kampo medicines improved cognitive impairment, cerebral blood flow, and BPSD.^{19–22} Moreover, the ameliorative effects of Kampo medicines have been demonstrated in various animal models of AD^{23–25} indicating that Kampo medicines are applicable as therapeutic agents for AD. In the present study, we examined the effects of orenge dokuto (OGT; 黃連解毒湯 huáng lián jiě dú tāng) and san'oshashinto (SST; 三黃瀉心湯 sān huáng xiè xīn tāng), Kampo formulae containing *Scutellariae Radix* (黃芩 huáng qín), on memory deficits and the aging-dependent activation of GSK-3 β in senescence-accelerated mouse-prone 8 (SAMP8), an animal model of aging and dementia. These formulae are often used to treat the symptoms of dementia in Japan²⁶; however, the mechanisms underlying their effects have not yet been elucidated. The present results showed that OGT and SST prevented aging-induced cognitive impairments by suppressing aging-dependent enhancements in GSK-3 β activity and CRMP2 phosphorylation. Our results provide a novel preventive strategy for dementia using Kampo medicines.

2. Materials and methods

2.1. Reagents

Baicalin, wogonin, and baicalein were obtained from Sigma-Aldrich (St. Louis, MO) and Wako Pure Chemical Industries, Ltd. (Osaka, Japan). All reagents and drugs used were of analytical grade.

2.2. Preparation and chemical profiling of OGT and SST

The following medicinal herbs, which conformed to Japanese Pharmacopoeia XVI, were purchased from Tochimoto tenkai-do (Osaka, Japan) to prepare OGT and SST. OGT was extracted from a mixture of 6.0 parts *Scutellariae Radix*, 4.0 parts *Coptidis Rhizoma* (黃連 huáng lián), 4.0 parts *Gardeniae Fructus* (山梔子 shān zhī zǐ), and 3.0 parts *Phellodendri Cortex* (黃柏 huáng bǎi). SST was extracted from a mixture of 6.0 parts *Scutellariae Radix*, 6.0 parts *Coptidis Rhizoma*, and 6.0 parts *Rhei Rhizoma* (大黃 dà huáng). The yields of the OGT and SST extracts were 7.71% and 7.95%, respectively. The chemical constituents of OGT and SST were analyzed using a Shimadzu LC-IT-TOF mass spectrometer equipped with an ESI interface. ESI parameters were as follows: source voltage, +4.5 kV (positive ion mode) or –3.5 kV (negative ion mode); capillary temperature, 200 °C; and nebulizer gas, 1.5 l/min. A Waters Atlantis T3 column (2.1 mm × 100 mm) was maintained at 40 °C. The mobile phase was a binary eluent of (A) 5 mM ammonium acetate solution and (B) acetonitrile under the following gradient conditions: 0–30 min; linear gradient from 10% to 100% B, and 30–40 min; isocratic at 100% B. The flow rate was

0.2 ml/min. Mass spectrometry data obtained from OGT and SST have been stored in the Wakan-Yaku DataBase system, Institute of Natural Medicine, University of Toyama (OGT: http://dentomed.toyama-wakan.net/en/information_on_experimental_kampo_extracts/Orenge dokuto-2016-KM/EXP004002; SST: http://dentomed.toyama-wakan.net/en/information_on_experimental_kampo_extracts/Sanoushashinto-2016-KM/EXP016002). Voucher specimens had been deposited at our institute.

2.3. Animals

Five-week-old male SAMP8 and SAM-resistant (SAMR1) mice were obtained from Japan SLC (Shizuoka, Japan). The housing room was maintained at 24 ± 1 °C with 65% humidity and a 12-h light-dark cycle (lights on: 07:30–19:30). Food and water were given *ad libitum*. All animal research procedures used in the present study were in accordance with the Guiding Principles for the Care and Use of Animals (NIH Publications No. 80-23, revised in 1996). The present study was also approved by the Institutional Animal Use and Care Committee of the University of Toyama. All surgery was performed under anesthesia, and all efforts were made to minimize suffering. The present study was conducted according to the experimental schedule described in [Supplementary Fig. S1](#).

2.4. Drug treatment

OGT (4250 mg/kg/day) or SST (4500 mg/kg/day) was administered intragastrically from the age of 6 months until all behavioral experiments were completed. In control groups, animals were treated with a water vehicle. These doses were approximately 30-fold higher than the typical daily doses for human therapy and in the ranges of herbal medicines that have been used in the study of animal models reported by our and other research groups.^{27,28}

2.5. Behavioral analysis

2.5.1. Nobel object recognition test (ORT)

ORT was conducted as previously described with minor modifications.²⁹ The apparatus consisted of a square arena (35 × 35 × 35 cm) with gray walls and a black floor. The objects for recognition had visual patterns or visually different shapes to be discriminated. ORT consisted of a sample trial and test trial. In the sample phase trial, each mouse was initially placed in the square arena with two identical objects, F1 and F2 (each of which was a 5.0 × 7.5 cm black cone), which were placed separately, and the mouse was allowed to freely explore the arena for five minutes. The total time that the mouse spent exploring each of the two objects was measured and the mouse was then returned to the home cage. In the test phase trial performed 30 min after the sample phase trial, one of the two objects was replaced by an identical copy (object F) and the other by a novel object (object N) and the total time that the mouse spent exploring each of the two objects was measured again. The performance of animals in these trials was video-recorded for later analyses and the exploration of an object was defined as directing the nose to the object at a distance of less than 2 cm according to previous studies. Mice that did not approach both objects during the 5-min observation period were excluded from the test trials. The time spent exploring each of the two objects was analyzed with SMART[®] ver. 2.5 (PanLab, SLU, Spain) with a tri-wise module to detect the head, center of mass, and base of the tail. The box arena and objects were cleaned with 75% ethanol between trials to prevent a build-up of olfactory cues.

2.5.2. Conditioned fear memory test (CFT)

CFT was performed using the protocol of Ebihara et al. with

minor modifications.³⁰ Briefly, the equipment for fear conditioning consisted of a transparent acrylic chamber (30 cm × 30 cm × 30 cm) and a stainless-steel grid floor equipped with an electric shock generator/scrambler SGS-002[®], CS Controller CSS-001[®], and Cycle Timer CMT[®] (Muromachi Kikai. Co. Ltd., Tokyo, Japan). The equipment was placed in a soundproof observation box (MC-050/CM, Muromachi Kikai, Co., Ltd., Tokyo, Japan) through which an auditory tone (Sonalert[®], Mallory Sonalert Products Inc., Indianapolis, IN, USA) was delivered to the animal. In the training trial, animals were placed individually into the chamber and allowed to explore freely for 3 min. They then received an acoustic tone (2.9 kHz, 20 s, 80 dB) that co-terminated with electric foot shocks (0.8 mA, 2 s). The tone-foot shock pairing was repeated 5 times with 1-min intervals. One minute after the final foot shock delivery, mice were returned to their home cage. Mice that did not respond to the foot shocks were excluded from the test trials. Contextual and auditory fear memories were examined 24 h and 6 days after the training trial, respectively. In the contextual memory test, mice were placed in the same chamber to provide contextual stimuli without an acoustic tone and allowed to move freely for 6 min. One minute after placing the animal in the chamber, freezing behavior during a 5-min period was recorded as an index of contextual-dependent fear memory. In measurements of auditory-dependent fear memory, mice were placed in another chamber for a total of 6 min. After a 3-min habituation period, the tone was delivered continuously for 3 min. Freezing behavior during the 3-min period was recorded as auditory-dependent fear memory. Animal behavior was video-recorded and analyzed automatically using the Smart[®] system. Freezing was defined as the absence of any movement, except for that related to respiration, and analyzed as a state with a movement speed no greater than 0.05 cm²/s.^{28,31}

2.6. Preparation of lysates

The cortex and hippocampus were obtained from each mouse and homogenized in protein lysis buffer [RIPA buffer (Cell Signaling Technology Inc., U.S.A.), protein inhibitor cocktail (Roche Diagnostics K. K., Japan), and 2 mM phenylmethylsulfonyl fluoride] using Tissuelyser[®] (Qiagen, Osaka, Japan), and centrifuged at 1500×g at 4 °C for 10 min. The protein concentrations of supernatants were measured using a BCA[™] protein assay kit (Thermo Scientific, Rockford, IL, USA). Protein extracts containing 5 µg/ml proteins were used in subsequent experiments.

2.7. Measurement of *in vivo* and *ex vivo* activities of GSK-3β

The activity of GSK-3β was measured using a kinase assay with two experimental paradigms: an *in vitro* analysis using recombinant active GSK-3β proteins (Sigma, St. Louis, MO, USA) and an *ex vivo* analysis using bio-samples extracted from animal brains after behavioral experiments. The kinase assay was conducted using an ADP-Glo[™] Kinase Assay Kit (Promega, WI, USA) according to the manufacturer's instructions. Briefly, 5 µl of kinase reaction solution contained 16 mM Tris-HCl (pH 7.5), 8 mM MgCl₂, 0.04 mg/ml bovine serum albumin, 0.4% DMSO, 2 mM β-mercaptoethanol, 0.2 mg/ml GSK3 substrate, 10 µM ATP, and 0.5 units of recombinant active GSK-3β proteins or 15 µg of protein extracts. The amount of protein was reduced to 1.5 µg in Lineweaver-Burk plot analysis. The kinase reaction solution was incubated at 25 °C for 1 h. Five microliters of ADP-Glo[™] Reagent was added to the reaction solution, which was then incubated at 25 °C for 1 h. Ten microliters of Kinase Detection Reagent was added to the reaction solution, and incubated at 25 °C for 1 h. Luminescence was measured on a microplate reader (FilterMax F5; Molecular Device, USA).

2.8. Western blotting

The phosphorylation of GSK-3β, tau, and CRMP2 was analyzed using Western blotting as previously described.²⁸ Briefly, we randomly selected four mice from each group. Protein lysates from the hippocampus and cortex were obtained as described above. Protein extracts containing 10 µg of protein were applied to SDS-polyacrylamide gels and electrophoresed. Separated proteins were transferred to a polyvinylidene difluoride membrane (Immuno-Blot[®] membrane, Bio-Rad Laboratories, Hercules, CA, USA). Blots were blocked with 2.5% bovine serum albumin in 0.1% Tween 20 containing TBS-T, and probed with the primary antibodies described below using a 1:1000 dilution at 4 °C overnight, followed by an incubation with an anti-rabbit or anti-mouse IgG antibody HRP-linked in a dilution of 1:2000 at room temperature for 2 h. After washing in TBS-T, chemiluminescence was detected using Immobilon[™] Western Chemiluminescent HRP Substrate (Millipore, Billerica, MA, USA). Immunoreactive bands were visualized and analyzed with ImageQuant LAS-4000 and ImageQuant TL[®] (GE Healthcare Japan, Tokyo, Japan).

The primary antibodies used were: an anti-GSK-3β rabbit monoclonal antibody, anti-phospho-GSK-3β (Ser9) rabbit monoclonal antibody, anti-phospho-tau (Ser396) rabbit monoclonal antibody, anti-phospho-CRMP2 (Thr514) rabbit monoclonal antibody, anti-CRMP2 rabbit monoclonal antibody, and anti-GAPDH mouse monoclonal antibody.

2.9. Statistical analysis

Data are expressed as the mean ± S.E.M. Data obtained in ORT were analyzed by the paired *t*-test for two groups according to a previous study. Data obtained in the fear conditioning test and neurochemical studies were analyzed by the Student's *t*-test for two groups or a one-way ANOVA followed by the Student–Newman–Keuls test for multiple comparisons. *P* values of <0.05 were considered to be significant. The analysis was conducted using SigmaPlot[®] ver 12.0 software (SYSTAT Software Inc., Richmond, CA, USA).

3. Results

3.1. OGT and SST ameliorated the non-spatial cognitive deficits of SAMP8

First, the object recognition test (ORT) was performed to assess the effects of OGT and SST on non-spatial cognitive deficits in SAMP8. Sample trials of ORT revealed no significant differences in the total time spent exploring two identical objects between each group (SAMR1: *t* = -0.485, *df* = 10, *p* = 0.638; SAMP8-vehicle: *t* = 1.352, *df* = 9, *p* = 0.209; SAMP8-OGT: *t* = 0.524, *df* = 10, *p* = 0.612; SAMP8-SST: *t* = 1.274, *df* = 9, *p* = 0.235) (Fig. 1A). In the test trials, SAMR1 spent a significantly longer time exploring a novel object than a familiar object (*t* = 2.357, *df* = 10, *P* < 0.05), indicating a preference for novelty. In contrast, SAMP8 showed no preference for the novel object (SAMP8-vehicle: *t* = 2.222, *df* = 9, *P* = 0.053). The treatment of SAMP8 with OGT or SST normalized novel object recognition behavior in this group, the animals in which spent a significantly longer time on the novel object than on the familiar object (SAMP8-OGT: *t* = 4.01, *df* = 10, *P* < 0.01; SAMP8-SST: *t* = 7.715, *df* = 9, *P* < 0.01) (Fig. 1B).

3.2. OGT and SST had no effects on the fear memory deficit in SAMP8

Next, we performed the conditioned fear memory test (CFT) in

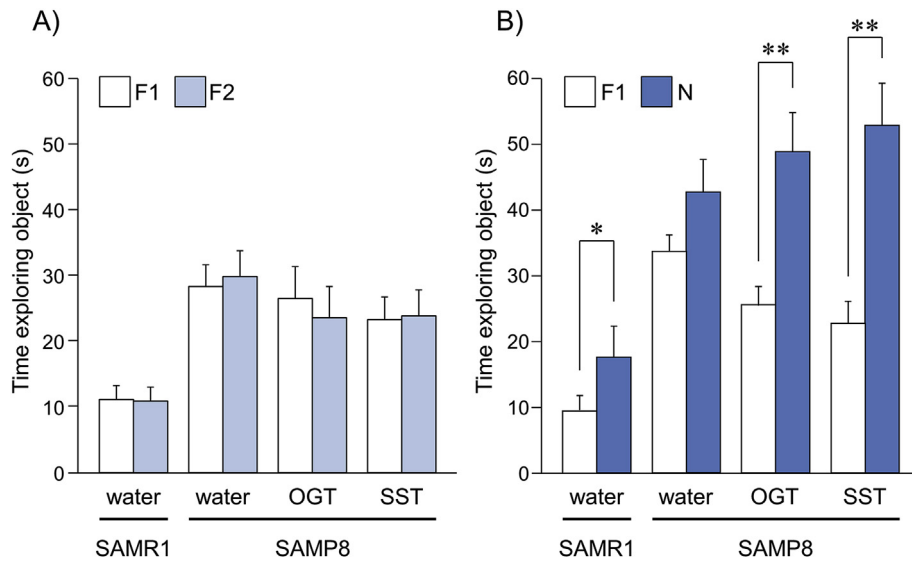


Fig. 1. Effects of OGT and SST on object recognition performance in SAMP8. The sample (A) and test (B) trials of the object recognition test (ORT) were conducted as described in the text. The numbers in each group were 11 (SAMR1-water), 10 (SAMP8-water), 11 (SAMP8-OGT), and 11 (SAMP8-SST). Each data point represents the mean ± S.E.M. *P < 0.05, **P < 0.01 vs. the time spent exploring F1 (paired t-test).

order to assess the effects of OGT and SST on long-term fear memory deficits in SAMP8 (Fig. 2). The freezing times of SAMP8 in the contextual (Fig. 2A) and auditory (Fig. 2B) memory tests were significantly less than those of SAMR1 (contextual: $t = 3.142$, $df = 19$, $p < 0.05$; auditory: $t = 2.443$, $df = 19$, $p < 0.05$). However, OGT and SST failed to improve context- and auditory-dependent fear memories (contextual: $F(2,28) = 1.002$, $p = 0.380$; auditory: $F(2,28) = 2.313$, $p = 0.118$).

3.3. OGT and SST inhibited age-dependent GSK-3β activation in SAMP8 cortex without phosphorylated regulation

After completing the behavioral experiments, we analyzed the

effects of OGT and SST on the *ex vivo* activities of GSK-3β in the brains of these animals. The activity of GSK-3β in the cortex was approximately 25% higher in SAMP8 than in age-matched SAMR1 ($t = -3.570$, $df = 6$, $p < 0.05$) (Fig. 3A1). Moreover, the elevation in GSK-3β activity was abolished in SAMP8 treated with OGT and SST [$F(2,9) = 8.281$, $p < 0.05$, SAMP8-vehicle vs. SAMP8-OGT: $p < 0.05$; SAMP8-vehicle vs. SAMP8-SST: $p < 0.05$] (Fig. 3A1). In contrast, no significant difference was observed in the hippocampal activity of GSK-3β between each group [SAMR1 vs. SAMP8: $t = 0.992$, $df = 6$, $p = 0.359$; among treatment: $F(2,9) = 0.0126$, $p = 0.988$] (Fig. 3A2). A significant difference was not noted in GSK-3β activity in the cortex when activity was analyzed at the age of 2 months ($t = 1.363$, $df = 6$, $p = 0.222$) (Fig. 3B). Next, the enzyme kinetics was analyzed

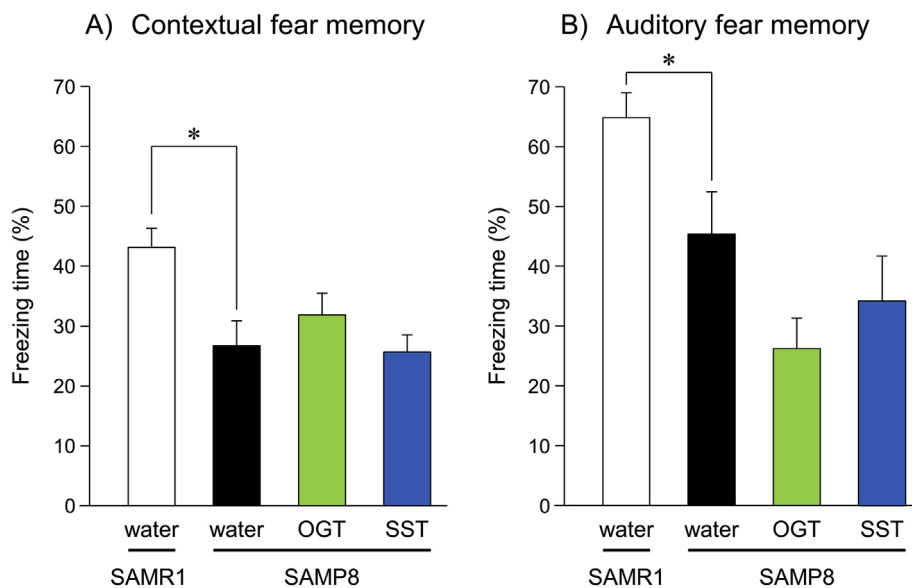


Fig. 2. Effects of OGT and SST on long-term fear memory deficits in SAMP8. The freezing times of animals under the contextual (A) and auditory (B) experimental conditions were measured as described in the text. OGT and SST were administered orally at doses of 4250 and 4500 mg/kg/day for 5 weeks before the test. The numbers of each group were 11 (SAMR1-water), 10 (SAMP8-water), 11 (SAMP8-OGT), and 10 (SAMP8-SST). Each data column represents the mean ± S.E.M. *P < 0.05 vs. SAMR1 group (Student's t-test). #p < 0.05 significantly different from the water-administered SAMP8 group (Student-Newman-Keuls test).

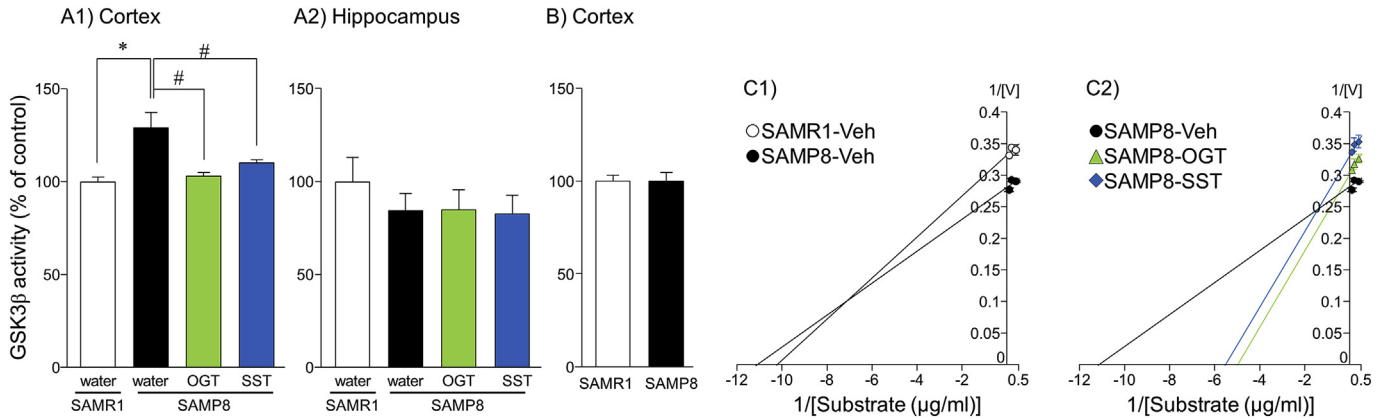


Fig. 3. Effects of OGT and SST administration on the *ex vivo* activity of GSK-3 β in the cortex and hippocampus of SAMP8. GSK-3 β activity was measured in cortical and hippocampal homogenate preparations obtained from SAMP8 and SAMR1 at the age of 8 (A1, 2) or 2 months (B). Each data column represents the mean \pm S.E.M. ($n = 4$). * $P < 0.05$ significantly different from SAMR1 (Student's *t*-test). # $P < 0.05$ significantly different from the SAMP8-vehicle group (Student-Newman-Keuls test). (C) Lineweaver-Burk plot of the GSK-3 β activity between SAMR1 and SAMP8 (C1) and GSK-3 β inhibition by OGT and SST in SAMP8 (C2). *V* represents the rate of enzyme reaction ($\mu\text{M}/\text{h}$). Each data point represents the mean \pm S.E.M. ($n = 3$).

with Lineweaver-Burk plot to determine the type of the age-dependent increase of GSK-3 β activity in SAMP8 or the inhibitory types by OGT and SST (Fig. 3C). In the GSK-3 β in the cortex of SAMP8, V_{max} increased from 3.015 to 3.558 but K_m decreased from 0.098 to 0.089, as compared with that of SAMR1 (Fig. 3C1). Moreover, OGT and SST showed mixed inhibition such that V_{max} decreased to 3.306 and 3.018 and K_m increased to 0.202 and 0.171, respectively (Fig. 3C2).

The expression levels of non-phosphorylated and Ser9-phosphorylated GSK-3 β in the cortex of SAMR1 and vehicle- and test drug-treated SAMP8 were measured by Western blotting (Fig. 4). No significant differences were found in the expression

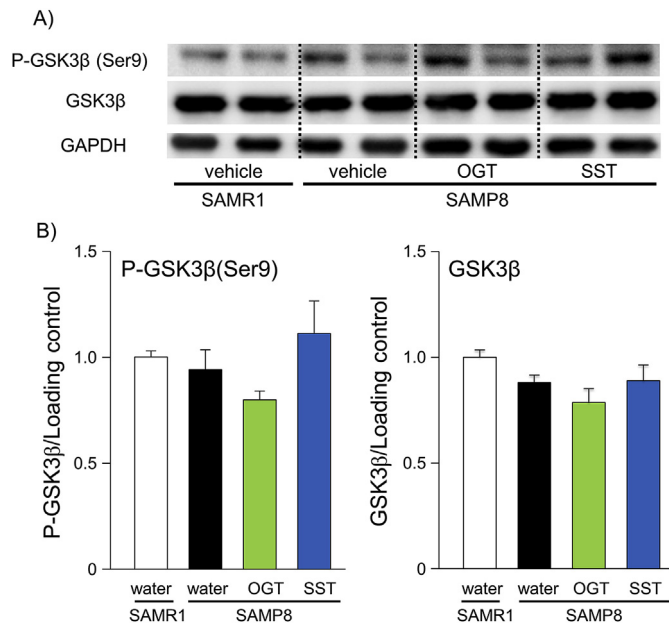


Fig. 4. Effects of OGT and SST on expression levels of GSK-3 β and phosphorylated GSK3 β (P-GSK-3 β) in the cortex of SAMP8. A) Typical photos indicating the levels of P-GSK-3 β , GSK-3 β , and GAPDH in the cortex obtained from SAMR1 and SAMP8 treated with water, OGT, and SST. Columns in each group represent biological replicates. B) Quantitative comparisons of the expression levels of P-GSK-3 β , GSK-3 β , and GAPDH among different groups. Each data column represents the mean \pm S.E.M. obtained from 4 brain samples. * $P < 0.05$ significantly different from SAMR1 (Student's *t*-test). # $P < 0.05$ significantly different from the SAMP8-vehicle group (Student-Newman-Keuls test).

levels of the P-GSK-3 β or GSK-3 β between SAMR1 and vehicle-treated SAMP8 (P-GSK-3 β : $t = 0.598$, $df = 6$, $p = 0.572$; GSK-3 β : $t = 2.421$, $df = 6$, $p = 0.052$). Moreover, the administration of OGT and SST had no effects on the expression levels of GSK-3 β or P-GSK-3 β in the cortex of SAMP8 [P-GSK-3 β : $F(2,9) = 2.151$, $P = 0.172$; GSK-3 β : $F(2,9) = 0.838$, $P = 0.464$] (Fig. 4).

3.4. OGT and SST inhibited the phosphorylation of CRMP2 but not tau in the cortex of SAMP8

We confirmed whether aging-dependent elevations in cortical GSK-3 β activity in SAMP8 affects the phosphorylation of the downstream molecules, tau and CRMP2, and, if so, how the administration of OGT and SST changes the levels of the phosphorylated forms of tau and CRMP2 in the cortex of SAMP8. Tau Ser396 phosphorylation in the cortex showed no significant differences between each group [SAMR1 v.s. SAMP8: $t = 0.511$, $df = 6$, $p = 0.627$; among treatments: $F(2,9) = 0.207$, $p = 0.816$] (Fig. 5A and B1). P-CRMP2 levels in the cortex were significantly higher in vehicle-treated SAMP8 than in SAMR1 ($t = -6.706$, $df = 6$, $p < 0.01$), and the administration of OGT and SST significantly decreased the elevated cortical level of P-CRMP2 in SAMP8 [$F(2,9) = 7.126$, $p = 0.014$, SAMP8-vehicle vs.SAMP8-OGT: $p = 0.014$; SAMP8-vehicle vs.SAMP8-SST: $p = 0.022$] without affecting the expression of CRMP2 [SAMR1 v.s. SAMP8: $t = 1.480$, $df = 6$, $p = 0.189$; among treatments: $F(2,9) = 0.817$, $p = 0.472$] (Fig. 5B2 and 3).

3.5. Flavonoid compounds contained in *Scutellariae Radix* inhibited GSK-3 β activity

Finally, we examined the inhibitory effects of GSK-3 β activity by active ingredients contained in OGT and SST. Among them, three flavonoid compounds, baicalin, wogonin, and baicalein, contained in *S. Radix* inhibited the *in vitro* activity of GSK-3 β in a concentration-dependent manner [baicalin: $F(3, 8) = 29.864$, $P < 0.01$; wogonin: $F(4, 10) = 11.445$, $P < 0.001$; baicalein: $F(4, 10) = 5.129$, $P = 0.016$] (Fig. 6 and Supplementary Fig. S2).

4. Discussion

The present study using ORT revealed that SAMP8 exhibited impaired object recognition performance, an index of short-term non-spatial working memory, in a manner that was reversed by

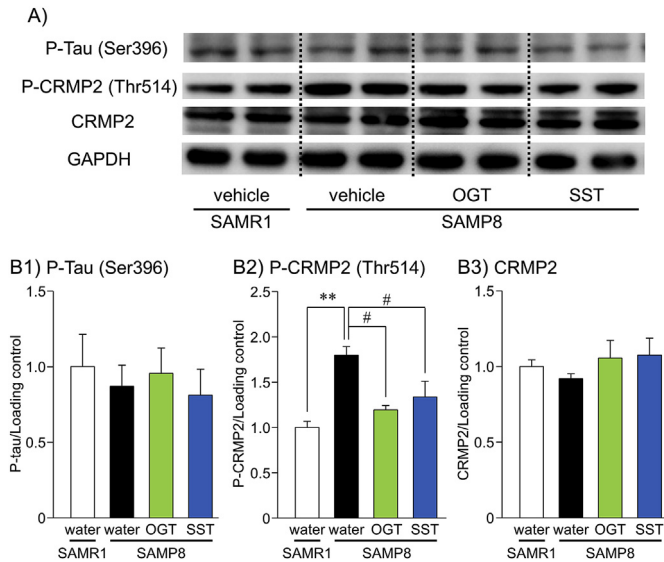


Fig. 5. Effects of OGT and SST on cortical levels of phospho-Tau (P-Tau) and phosphor-CRMP2 (P-CRMP2) in the cortex of SAMR1 and SAMP8. A) Typical photos indicating the levels of P-Tau, P-CRMP2, and total CRMP2 in the cortex obtained from SAMR1 and SAMP8 treated with water, OGT, and SST. Columns in each group represent biological replicates. B) Quantitative comparisons of the levels of P-tau (B1), P-GSK-3 β (B2), and total CRMP2 (B3). Each data column represents the mean \pm S.E.M. obtained from 4 brain samples. * $P < 0.05$ significantly different from SAMR1 (Student's *t*-test). # $P < 0.05$ significantly different from the SAMP8-vehicle group (Student-Newman-Keuls test).

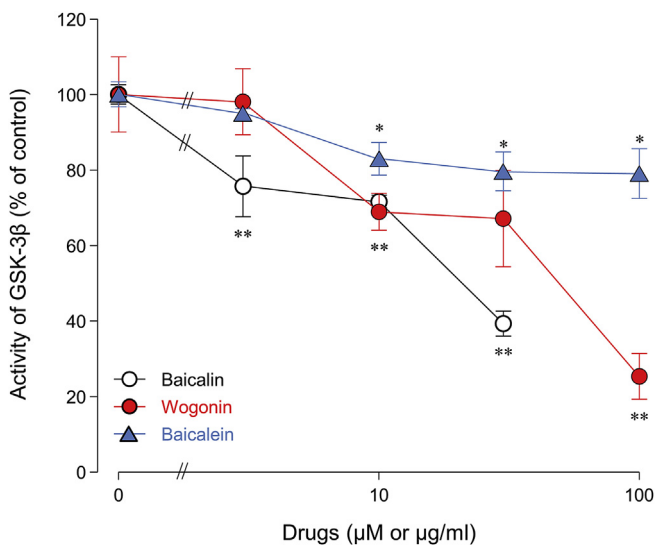


Fig. 6. Effects of baicalin, wogonin, and baicalein, flavonoids contained in OGT and SST, on the activity of recombinant GSK-3 β . The activities of recombinant GSK-3 β were measured using an ADP-Glo™ Kinase Assay Kit. Each data point represents the mean \pm S.E.M. ($n = 3$). * $P < 0.05$, ** $P < 0.01$ significantly different from the vehicle control (Student-Newman-Keuls test).

the administration of OGT and SST. Moreover, the cognitive deficit in SAMP8 was accompanied by significant elevations in cortical GSK-3 β activity. Since no significant differences were observed in GSK-3 β activity in SAMP8 in 2-month-old SAMP8 or in hippocampal tissues in SAMP8, our results provide at least two important suggestions. The increase in cortical GSK-3 β activity in SAMP8 may have occurred in an aging-dependent manner and contributed to the development of non-spatial short-term working memory deficits in this animal model. Furthermore, we may infer that the administration of OGT and SST suppresses aging-dependent

increases in cortical GSK-3 β activity, thereby preventing aging-induced non-spatial cognitive deficits.

Non-spatial memory detected in ORT is known to be related to short-term episodic memory in humans,³² which is impaired in the early stages of dementia.³³ The entorhinal area is essential for short-term episodic memory to function normally.³⁴ Moreover, evidence indicates that neurofibrillary tangles are formed in the entorhinal cortex in the early stages of AD, and spread to other parts as the disease progresses.³⁵ Collectively, the present results allow us to infer that the elevated activity of GSK-3 β impairs the function of the entorhinal area adjacent to the cortex in the early stages of AD, thereby contributing to the progression of the disease, and also that OGT and SST may be able to suppress early AD progression by inhibiting GSK-3 β in the cortex or entorhinal area.

In contrast to short-term working memory deficits in ORT, long-term memory deficits in SAMP8 in CFT were not susceptible to the treatment with OGT and SST. Furthermore, GSK-3 β activity in the hippocampus was similar among the animal groups regardless of whether they were treated with OGT and/or SST. These results indicate that the contribution of hippocampal GSK-3 β activity to long-term fear memory deficits is negligible under our experimental conditions.

Although the mechanisms underlying aging-dependent changes in GSK-3 β activity currently remain unclear, it is suggested that the complicated factors are involved, because that Lineweaver-Burk plot revealed that GSK-3 β of SAMP8 has higher both of a maximum rate of the enzyme reaction and an affinity for GSK-3 β substrate than that of SAMR1. For example, the aging-induced activation of GSK-3 β in the cortex may be attributable to functional changes in endogenous molecules with regulatory roles in GSK-3 β activity. Evidence indicates that GSK-3 β forms a complex with other endogenous molecules such as Axin, adenomatous polyposis coli, casein kinase α , and β -catenin and may be regulated by a Wnt signaling cascade.³⁶ Ye et al.³⁷ previously reported that GSK-3 β was activated by attenuating the Wnt2 signal, which accompanies cellular senescence. Furthermore, the down-regulation of an inactivation system for GSK-3 β activity may be caused by aging, which apparently increases the activity of this enzyme in the cortex. Other kinases such as Akt reportedly convert GSK-3 β to an inactive form by phosphorylating the Ser9 residue of the GSK-3 β protein.¹⁰ However, this does not appear to be likely because no significant differences were observed in P-GSK-3 β levels in the cortex between SAMP8 and SAMR1. Further investigations are needed in order to elucidate the exact mechanisms by which aging activates the cortical activity of GSK-3 β .

Tau and CRMP2 are substrates for the activity of GSK-3 β and are involved in stabilizing the microtubules of nerve cells.^{3,15} Furthermore, the phosphorylation of these proteins caused by the activity of GSK-3 β is known to be closely related to dysfunctional neuronal transmission and cognitive deficits in patients with dementia.^{10,11} The present results revealed that the cortical levels of P-CRMP2, but not P-tau were significantly higher in 8-month-old SAMP8 than in age-matched SAMR1. These results not only indicate that the aging-induced activation of GSK-3 β in the cortex links more preferentially to the phosphorylation of CRMP2 than tau protein, but also suggest that the link between GSK-3 β activation and CRMP2 phosphorylation mainly contributes to memory deficits in a model of aging. Moreover, since the increase in cortical P-CRMP2 levels was attenuated in SAMP8 treated with OGT and SST, the administration of OGT and SST appears to prevent aging-induced working memory deficits by suppressing GSK-3 β activation and/or the link between GSK activation and GSK-3 β -mediated CRMP2 phosphorylation in the cortex. This appears to be supported by studies using other natural products. Wang et al. reported that curcumin, a bioactive component of *Curcuma longa*, ameliorated

β -amyloid-induced cognitive dysfunction by suppressing the hyper-phosphorylation of CRMP2.¹⁸ Furthermore, in CRMP2 phosphorylation-deficient knock-in mice, β -amyloid failed to induce memory deficits in the ORT.³⁸

Several researchers have demonstrated that baicalin, wogonin, and baicalein, which are flavonoid constituents of *S. Radix* contained in OGT and SST, exert anti-dementia effects in several animal models of AD^{39–41}. Collectively, our *in vitro* results suggest that these flavonoids contribute, at least in part, to the suppressive effects of OGT and SST on aging-induced GSK-3 β activation as well as on aging-induced working memory deficits in mice. However, since the inhibition of *in vitro* GSK-3 β activity by baicalin, wogonin, and baicalein was very limited, we cannot exclude the possibility that OGT- and SST-derived chemical constituents other than these flavonoids also contribute to the effects of OGT and SST observed in the present study. The fact that OGT and SST revealed the mixed inhibition in the Lineweaver-Burk plot also suggests that multiple compounds are involved in the inhibition of GSK-3 β . This possibility is currently being investigated in our laboratory.

5. Conclusion

The present study demonstrated that the administration of OGT and SST ameliorated aging-induced episodic memory deficits, possibly by inhibiting the aging-dependent activation of GSK-3 β as well as subsequent CRMP2 phosphorylation. Thus, these Kampo formulae may offer a new preventive/therapeutic strategy from the early stages of dementia.

Conflicts of interest

The authors and contributors of this work declare no conflicts of interest.

Acknowledgments

This study was in part supported by a Grant-in-Aid for Scientific Research from the Japan Society for the Promotion of Science to HF (JP25860075), a 2012 Grant-in-Aid from Mochida Memorial Foundation for Medical and Pharmaceutical Research (HF), a 2012 Grant-in-Aid from Tamura Science and Technology Foundation (HF), and 2017 Director Leadership Expenses, University of Toyama (HF).

Appendix A. Supplementary data

Supplementary data to this article can be found online at <https://doi.org/10.1016/j.jtcme.2018.12.001>.

References

- Hardy J, Selkoe DJ. The amyloid hypothesis of Alzheimer's disease: progress and problems on the road to therapeutics. *Science*. 2002;297(5580):353–356.
- Serrano-Pozo A, Froesch MP, Masliah E, Hyman BT. Neuropathological alterations in Alzheimer disease. *Cold Spring Harb Perspect Med*. 2011;1(1):a006189.
- Plattner F, Angelo M, Giese KP. The roles of cyclin-dependent kinase 5 and glycogen synthase kinase 3 in tau hyperphosphorylation. *J Biol Chem*. 2006;281(35):25457–25465.
- Bloom GS. Amyloid- β and tau: the trigger and bullet in Alzheimer disease pathogenesis. *JAMA Neurol*. 2014;71(4):505–508.
- Beurel E, Grieco SF, Joje RS. Glycogen synthase kinase-3 (GSK3): regulation, actions, and diseases. *Pharmacol Ther*. 2015;148:114–131.
- Park SB, Kwok JB, Loy CT, et al. Paclitaxel-induced neuropathy: potential association of *MAPT* and *GSK3B* genotypes. *BMC Canc*. 2014;14:993.
- Rydbirk R, Elfving B, Andersen MD, et al. Cytokine profiling in the prefrontal cortex of Parkinson's Disease and Multiple System Atrophy patients. *Neurobiol Dis*. 2017;106:269–278.
- Bharathy N, Svalina MN, Settlemeyer TP, et al. Preclinical testing of the glycogen synthase kinase-3 β inhibitor tideglusib for rhabdomyosarcoma. *Oncotarget*. 2017;8(38):62976–62983.
- Lim YW, Yoon SY, Choi JE, et al. Maintained activity of glycogen synthase kinase-3 β despite of its phosphorylation at serine-9 in okadaic acid-induced neurodegenerative model. *Biochem Biophys Res Commun*. 2010;395(2):207–212.
- Orellana AM, Vasconcelos AR, Leite JA, et al. Age-related neuroinflammation and changes in AKT-GSK-3 β and WNT/ β -CATENIN signaling in rat hippocampus. *Aging (Albany NY)*. 2015;7(12):1094–1111.
- Xu ZP, Yang SL, Zhao S, et al. Biomarkers for early diagnostic of mild cognitive impairment in type-2 diabetes patients: a multicentre, retrospective, nested case-control study. *EBioMedicine*. 2016;5:105–113.
- Hensley K, Venkova K, Christov A, Gunning W, Park J. Collapsin response mediator protein-2: an emerging pathologic feature and therapeutic target for neurodegeneration. *Mol Neurobiol*. 2011;43(3):180–191.
- Charrier E, Reibel S, Rogemond V, Aguera M, Thomasset N, Honnorat J. Collapsin response mediator proteins (CRMPs): involvement in nervous system development and adult neurodegenerative disorders. *Mol Neurobiol*. 2003;28(1):51–64.
- Yoshimura T, Kawano Y, Arimura N, Kawabata S, Kikuchi A, Kaibuchi K. GSK-3 β regulates phosphorylation of CRMP-2 and neuronal polarity. *Cell*. 2005;120(1):137–149.
- Gu Y, Hamajima N, Ihara Y. Neurofibrillary tangle-associated collapsin response mediator protein-2 (CRMP-2) is highly phosphorylated on Thr-509, Ser-518, and Ser-522. *Biochemistry*. 2000;39(15):4267–4275.
- Xing H, Lim YA, Chong JR, et al. Increased phosphorylation of collapsin response mediator protein-2 at Thr514 correlates with β -amyloid burden and synaptic deficits in Lewy body dementias. *Mol Brain*. 2016;9(1):84.
- Cole AR, Noble W, van Aalten L, et al. Collapsin response mediator protein-2 hyperphosphorylation is an early event in Alzheimer's disease progression. *J Neurochem*. 2007;103(3):1132–1144.
- Wang Y, Yin H, Li J, et al. Amelioration of β -amyloid-induced cognitive dysfunction and hippocampal axon degeneration by curcumin is associated with suppression of CRMP-2 hyperphosphorylation. *Neurosci Lett*. 2013;557(Pt B):112–117.
- Le Bars PL, Katz MM, Berman N, Itil TM, Freedman AM, Schatzberg AF. A placebo-controlled, double-blind, randomized trial of an extract of Ginkgo biloba for dementia. North American Egb study group. *J Am Med Assoc*. 1997;278(16):1327–1332.
- Terasawa K, Shimada Y, Kita T, et al. Choto-san in the treatment of vascular dementia: a double-blind, placebo-controlled study. *Phytomedicine*. 1997;4(1):15–22.
- Iwasaki K, Kobayashi S, Chimura Y, et al. A randomized, double-blind, placebo-controlled clinical trial of the Chinese herbal medicine "ba wei di huang wan" in the treatment of dementia. *J Am Geriatr Soc*. 2004;52(9):1518–1521.
- Iwasaki K, Satoh-Nakagawa T, Maruyama M, et al. A randomized, observer-blind, controlled trial of the traditional Chinese medicine *Yi-Gan San* for improvement of behavioral and psychological symptoms and activities of daily living in dementia patients. *J Clin Psychiatr*. 2005;66(2):248–252.
- Zhao Q, Yokozawa T, Tsuneyama K, et al. Chotosan (*Diaoteng San*)-induced improvement of cognitive deficits in senescence-accelerated mouse (SAMP8) involves the amelioration of angiogenic/neurotrophic factors and neuroplasticity systems in the brain. *Chin Med*. 2011;6:33.
- Zhao Q, Matsumoto K, Tsuneyama K, et al. Diabetes-induced central cholinergic neuronal loss and cognitive deficit are attenuated by tacrine and a Chinese herbal prescription, kangen-karyu: elucidation in type 2 diabetes *db/db* mice. *J Pharmacol Sci*. 2011;117(4):230–242.
- Zhao Q, Niu Y, Matsumoto K, et al. Chotosan ameliorates cognitive and emotional deficits in an animal model of type 2 diabetes: possible involvement of cholinergic and VEGF/PDGF mechanisms in the brain. *BMC Complement Altern Med*. 2012;12:188.
- Araki G. The effects of orengeodokuto on senile dementia (in Japanese). *Theapeutic Research*. 1994;15:986–994.
- Fujiwara H, Takayama S, Iwasaki K, et al. Yokukansan, a traditional Japanese medicine, ameliorates memory disturbance and abnormal social interaction with anti-aggregation effect of cerebral amyloid β proteins in amyloid precursor protein transgenic mice. *Neuroscience*. 2011;180:305–313.
- Fujiwara H, Han Y, Ebihara K, et al. Daily administration of yokukansan and keishito prevents social isolation-induced behavioral abnormalities and down-regulation of phosphorylation of neuroplasticity-related signaling molecules in mice. *BMC Complement Altern Med*. 2017;17(1):195.
- Yamada M, Hayashida M, Zhao Q, et al. Ameliorative effects of yokukansan on learning and memory deficits in olfactory bulbectomized mice. *J Ethnopharmacol*. 2011;135(3):737–746.
- Ebihara K, Fujiwara H, Awale S, et al. Decrease in endogenous brain allopregnanolone induces autism spectrum disorder (ASD)-like behavior in mice: a novel animal model of ASD. *Behav Brain Res*. 2017;334:6–15.
- Okada R, Fujiwara H, Mizuki D, Araki R, Yabe T, Matsumoto K. Involvement of dopaminergic and cholinergic systems in social isolation-induced deficits in social affiliation and conditional fear memory in mice. *Neuroscience*. 2015;299:134–145.
- Bertaina-Anglade V, Enjuanes E, Morillon D, Drieu la Rochelle C. The object recognition task in rats and mice: a simple and rapid model in safety pharmacology to detect amnesic properties of a new chemical entity. *J Pharmacol Toxicol Methods*. 2006;54(2):99–105.
- Saunders NL, Summers MJ. Attention and working memory deficits in mild cognitive impairment. *J Clin Exp Neuropsychol*. 2010;32(4):350–357.

34. Trivedi MA, Stoub TR, Murphy CM, et al. Entorhinal cortex volume is associated with episodic memory related brain activation in normal aging and amnesic mild cognitive impairment. *Brain Imaging Behav.* 2011;5(2):126–136.
35. Gómez-Isla T, Price JL, McKeel Jr DW, Morris JC, Growdon JH, Hyman BT. Profound loss of layer II entorhinal cortex neurons occurs in very mild Alzheimer's disease. *J Neurosci.* 1996;16(14):4491–4500.
36. Inestrosa NC, Varela-Nallar L, Grabowski CP, Colombres M. Synaptotoxicity in Alzheimer's disease: the *Wnt* signaling pathway as a molecular target. *IUBMB Life.* 2007;59(4-5):316–321.
37. Ye X, Zerlanko B, Kennedy A, Banumathy G, Zhang R, Adams PD. Down-regulation of Wnt signaling is a trigger for formation of facultative heterochromatin and onset of cell senescence in primary human cells. *Mol Cell.* 2007;27(2):183–196.
38. Isono T, Yamashita N, Obara M, et al. Amyloid- β_{25-35} induces impairment of cognitive function and long-term potentiation through phosphorylation of collapsin response mediator protein 2. *Neurosci Res.* 2013;77(3):180–185.
39. Lee HW, Ryu HW, Kang MG, et al. Potent inhibition of monoamine oxidase A by decursin from *Angelica gigas* Nakai and by wogonin from *Scutellaria baicalensis* Georgi. *Int J Biol Macromol.* 2017;97:598–605.
40. Zhang SQ, Obregon D, Ehrhart J, et al. Baicalein reduces β -amyloid and promotes nonamyloidogenic amyloid precursor protein processing in an Alzheimer's disease transgenic mouse model. *J Neurosci Res.* 2013;91(9):1239–1246.
41. Chen C, Li X, Gao P, et al. Baicalin attenuates alzheimer-like pathological changes and memory deficits induced by amyloid β_{1-42} protein. *Metab Brain Dis.* 2015;30(2):537–544.